



1 **Influence of climate variability, fire and phosphorus limitation on the**
2 **vegetation structure and dynamics in the Amazon-Cerrado border**

3

4 Emily Ane Dionizio da Silva¹, Marcos Heil Costa¹, Andrea Almeida Castanho², Gabrielle Ferreira Pires¹,
5 Beatriz Schwantes Marimon³, Ben Hur Marimon-Junior³, Eddie Lenza³, Fernando Martins Pimenta¹,
6 Xiaojuan Yang⁴, Atul K. Jain⁵

7

8 ¹ Department of Agricultural Engineering, Federal University of Viçosa (UFV), Viçosa, MG, Brazil

9 ² The Woods Hole Research Center, 149 Woods Hole Rd., Falmouth, MA USA

10 ³ Federal University of Mato Grosso, Nova Xavantina Campus, Nova Xavantina, MT, Brazil

11 ⁴ Oak Ridge National Laboratory, Oak Ridge, TN, USA

12 ⁵ Department of Atmospheric Sciences, University of Illinois at Urbana-Champaign

13

14 Correspondence to: Emily Ane D. da Silva (emilyy.ane@gmail.com)

15



16 **Abstract**

17 Climate, fire and soil nutritional limitation are important elements that affect the vegetation
18 dynamics in areas of forest-savanna transition. In this paper, we use the dynamic vegetation model
19 INLAND to evaluate the influence of inter-annual climate variability, fire and phosphorus (P) limitation
20 on the Amazon-Cerrado transitional vegetation structure and dynamics. We assess how each
21 environmental factor affects the net primary production, leaf area index and aboveground biomass (AGB),
22 and compare the AGB simulations of observed AGB map. We used two climate datasets – the 1960-1990
23 average seasonal climate and the 1948 to 2008 inter-annual climate variability, two regional datasets of
24 total soil P content in soil, based on regional (field measurements) and global data and the INLAND fire
25 module. Our results show that inter-annual climate variability, P limitation and fire occurrence gradually
26 improve simulated vegetation types and these effects are not homogeneous along the
27 latitudinal/longitudinal gradient showing a synergistic effect among them. In terms of magnitude, the
28 effect of fire is stronger, and is the main driver of vegetation changes along the transition. The nutritional
29 limitation, in turn, is stronger than the effect of inter-annual climate variability acting on the transitional
30 ecosystems dynamics. Overall, INLAND typically simulates more than 80% of the AGB variability in
31 the transition zone. However, the AGB in many places is clearly not well simulated, indicating that
32 important soil and physiological factors in the Amazon-Cerrado border, such as lithology and water table
33 depth, carbon allocation strategies and mortality rates, still need to be included in the model.



34 **1 Introduction**

35 The Amazon and Cerrado are the two largest and most important phytogeographical domains in
36 South America. The Amazon forest has been globally recognized and distinguished not only for its
37 exuberance in diversity and species richness, but also for playing an important role in the global climate
38 by regulating water (Bonan, 2008; Pires and Costa, 2013) and heat fluxes (Shukla et al., 1990; Rocha et
39 al., 2004; Roy et al., 2002). The Cerrado is recognized worldwide for being the richest savanna in the
40 world (Myers et al., 2000; Klink and Machado, 2005). It is characterized by different physiognomies,
41 ranging from sparse physiognomies to dense woodland formations, and the latter are commonly mixed
42 with Amazon rainforest forming transitional areas. The Amazon-Cerrado transition extends for 6270 km
43 from northeast to southwest in Brazil, and the ecotonal vegetation around this transition is a mix of the
44 characteristics of the tropical forest and the savanna (Torello-Raventos et al., 2013).

45 Gradients of seasonal rainfall and water deficit, fire occurrence, herbivory and low fertility of the
46 soil have been reported as the main factors that characterize the transition between forest and savanna
47 globally (Lehmann et al., 2011; Hoffman et al., 2012; Murphy and Bowman, 2012). However, few studies
48 have evaluated the individual and combined effects of these factors on Brazilian ecosystems ecotones
49 (Marimon-Junior and Haridasan, 2005; Elias et al., 2013; Vourtilis et al., 2013).

50 It is challenging to assess the degree of interaction among these various environmental factors in
51 the transitional region and to infer how each one influences the distribution of the regional vegetation. In
52 this case, Dynamic Global Vegetation Models (DGVMs) can be powerful tools to isolate the influences
53 of climate, fire and nutrients, therefore helping to understand their large-scale effects on vegetation
54 (House et al., 2003; Favier et al., 2004; Hirota et al., 2010; Hoffman et al., 2012).



55 Previous modelling studies using DGVMs that investigate climate effects in the Amazon indicate
56 that the rainforest could experience changes in rainfall patterns which would either transform the forest
57 into an ecosystem with more sparse vegetation – similar to a savanna, what has been called as the
58 "savannization of the Amazon" (Shukla et al., 1990; Cox et al., 2000; Oyama and Nobre, 2003; Betts et
59 al., 2004; Cox et al., 2004; Salazar et al., 2007) - or to a seasonal forest (Malhi et al., 2009; Pereira et al.,
60 2012; Pires and Costa, 2013). These studies had great importance to the improvement of terrestrial
61 biosphere modeling, but they neglect two important processes in tropical ecosystem dynamics: fire
62 occurrence and nutrient limitation, particularly the P limitation.

63 In tropical ecosystems, fire plays an important ecological role and influences the productivity, the
64 biogeochemical cycles and the dynamics in the transitional biomes, not only by changing the phenology
65 and physiology of plants, but also by modifying the competition among trees and lower canopy plants
66 such as grasses, shrubs and lianas. Fire occurrence, depending on its frequency and intensity, may increase
67 the mortality of trees and transform an undisturbed forest into a disturbed and flammable one (House et
68 al., 2003; Hirota et al., 2010; Hoffmann et al., 2012). Fires also affect the dynamics of nutrients in the
69 savanna ecosystem, changing mainly the N:P relationship and P availability in the soil (Nardoto et al.
70 2006).

71 Studies suggest that P is the main limiting nutrient within tropical forests (Malhi et al., 2009;
72 Mercado et al., 2011; Quesada et al., 2012) unlike the temperate forests. Phosphorus (P) is a nutrient that
73 is easily adsorbed by soil minerals due to the large amount of iron and aluminum oxides in the Amazon
74 and Cerrado acidic and strongly weathered soils (Dajoz, 2005; Goedert, 1986). In the tropics, the warm
75 and wet climate favors the high biological activity in the soil and the litter decomposition, not limiting



76 the nitrogen for plant fixation. In Cerrado, higher soil fertility is related to regions with greater woody
77 plants abundance and less grass cover, similarly to the features found in the Amazon rainforest (Moreno
78 et al., 2008; Vourtilis et al., 2013; Veenendaal et al., 2015). However, the phosphorus limitation is often
79 neglected by DGVMs. which usually assume unlimited P availability and consider nitrogen as the main
80 limiting nutrient. However, N is not a limiting nutrient for trees in the tropics (Davidson et al. 2004),
81 while P availability affects the trees dynamics.

82 In principle, in transitional forests, where the climate is intermediate between wet and seasonally
83 dry, the heterogeneous structure and phenology make it difficult to represent these forests in models. The
84 Amazon-Cerrado border is the result of the expansion and contraction of the Cerrado into the forest (see
85 Marimon et al., 2006; Morandi et al., 2016), especially in the Mato Grosso state, where extreme events,
86 such as intense droughts, influence the vegetation dynamics (Marimon et al., 2014) and the nutrient
87 (Oliveira et al., *in press*) and carbon cycling (Valadão et al., 2016).

88 Currently, no model has demonstrated to be able to accurately simulate the vegetation transition
89 between Amazon and Cerrado. A better understanding of the main drivers that determine the distribution
90 of different vegetation physiognomies in the region is crucial for more reliable simulations of the
91 transitional tropical ecosystems in future climate scenarios.

92 In this paper we use the dynamic vegetation model INLAND (Integrated Model of Land Surface
93 Processes) to evaluate the influence of inter-annual climate variability, fire occurrence and P limitation
94 in the Amazon-Cerrado transitional vegetation dynamics and structure. We assess how each element
95 affects the net primary production (NPP), leaf area index (LAI) and aboveground biomass (AGB) and
96 compare the model simulated AGB to observed AGB data. The results presented here are important to



97 build models that accurately represent the transition vegetation, and show the need to include the spatial
98 variability of eco-physiological parameters in these areas.

99 **2 Materials and methods**

100 **2.1 Study Area**

101 The present study focuses on the Amazon-Cerrado transition (Figure 1). We use the official
102 delimitation of the Brazilian biomes proposed by IBGE (2004), and define five transects along the
103 transition border. Transects 1 to 4 are established considering approximately 330 km into the Amazon
104 and 330 km into the Cerrado domain, while Transect 5 is 880 km long on the southern Amazon-Cerrado
105 border. The transects are located as follows: Transect 1 (T1, 43°- 49°W; 5°- 7°S), Transect 2 (T2, 46°-
106 51° W; 7°-9S), Transect 3 (T3, 48°-54° W; 9°-11° S), Transect 4 (T4, 49° - 55° W; 11°-13° S), and
107 Transect 5 (T5, 53° - 61° W; 13°-15° S) (Figure 1).

108 **2.2 Description of the INLAND Surface Model**

109 The Integrated Model of Land Surface Processes (INLAND) is the land-surface component of the
110 Brazilian Earth System Model (BESM). INLAND is based on the IBIS model (Integrated Biosphere
111 Simulator, Foley et al., 1996; Kucharik et al., 2000), which considers changes in the composition and
112 structure of vegetation in response to the environment and incorporates important aspects of biosphere-
113 atmosphere interactions. The model simulates the exchanges of energy, water, carbon and momentum
114 between soil-vegetation-atmosphere. These processes are organized in a hierarchical framework and
115 operate at different time steps, ranging from 60 minutes to 1 year, coupling ecological, biophysical and
116 physiological processes. The vegetation structure is represented by two layers: upper (arboreal PFTs) and



117 lower (no arboreal PFTs, shrubs and grasses) canopies, and the composition is represented by 12 plant
118 functional types (PFTs) (e.g., tropical broadleaf evergreen trees or C4 grasses, among several others). The
119 photosynthesis and respiration processes are simulated in a mechanistic manner using the Ball-Berry-
120 Farquhar model (details in Foley et al., 1996). The vegetation phenology module simulates the processes
121 such as budding and senescence based on empirically-based temperature thresholds for each PFT. The
122 dynamic vegetation module computes the following variables yearly for each PFT: gross and net primary
123 productivity (GPP and NPP), changes in AGB pools, simple mortality disturbance processes and resultant
124 LAI, thus allowing vegetation type and cover to change with time. The partitioning of the NPP for each
125 PFT resolves carbon in three AGB pools: leaves, stems and fine roots. The LAI of each PFT is obtained
126 by simply dividing leaf carbon by specific leaf area, which in INLAND is considered fixed (one value)
127 for each PFT.

128 INLAND has eight soil layers to simulate the diurnal and seasonal variations of heat and moisture.
129 Each layer is described in terms of soil temperature, volumetric water content and ice content (Foley et
130 al., 1996; Thompson and Pollard, 1995). Furthermore, all of these processes are influenced by soil texture
131 and amount of organic matter within the soil profile.

132 Considering these aspects of vegetation dynamics and soil physical properties the model can
133 simulate plant competition for light and water between trees, shrubs and grasses through shading and
134 differences in water uptake (Foley et al., 1996). These PFTs can coexist within a grid cell and their annual
135 LAI values indicate the dominant vegetation type within a grid cell. For example, the dominant vegetation
136 type is a Tropical Evergreen Forest if the PFT tropical broadleaf evergreen tree has an annual mean upper
137 canopy LAI (LAI_{upper}) above $2.5 \text{ m}^2 \text{ m}^{-2}$. On the other hand, the dominant vegetation type is a Tropical



138 Deciduous Forest if the tropical broadleaf drought-deciduous tree has an annual mean LAI_{upper} above
139 $2.5 \text{ m}^2 \text{ m}^{-2}$. Where total tree LAI (LAI_{upper}) is between 0.8 and $2.5 \text{ m}^2 \text{ m}^{-2}$, dominant vegetation type is
140 savanna, and LAI_{upper} values smaller than $0.8 \text{ m}^2 \text{ m}^{-2}$ characterize a grassland vegetation type.

141 We assume that the vegetation types Tropical Evergreen Forest and the Tropical Deciduous Forest
142 in INLAND represent the Amazon rainforest, while Savanna and Grasslands represent the Cerrado.
143 Savanna would be equivalent to the Cerrado physiognomies *Cerradão* and *Cerrado sensu strictu*, while
144 Grasslands would be equivalent to the physiognomies *Campo sujo* and *Campo Limpo* (*sensu* Ribeiro and
145 Walter, 2008).

146 The soil chemical properties are represented by the carbon, nitrogen and phosphorus. The carbon
147 cycle is simulated through vegetation, litter and soil organic matter, where the biogeochemical module is
148 similar to the CENTURY model (Parton et al., 1993; Verberne et al., 1990). The amount of C existing in
149 the first meter of soil is divided into different compartments characterized by their residence time, which
150 can vary in an interval of hours for microbial AGB and organic matter to several years for lignin. The
151 model considers only the soil N transformations and carbon decomposition, but the N cycle is not fully
152 simulated and N does not influence the vegetation productivity, i.e., there is a fixed C:N ratio. P is used
153 only to limit the gross primary productivity. The total P available in the soil (P_{total}) is used to estimate the
154 maximum capacity of carboxylation by the Rubisco enzyme (V_{max}) through a linear relationship.

$$155 \quad V_{max} = 0.1013 P_{total} + 30.037 \quad (1)$$

156 where V_{max} and P_{total} are given in $\mu\text{molCO}_2 \text{ m}^{-2} \text{ s}^{-1}$ and mg kg^{-1} , respectively. This equation has been
157 developed by Castanho et al. (2013) based on data for tropical evergreen and deciduous trees, and is
158 applied only to these two PFTs in the model.



159 INLAND also contains a fire module, from the Canadian Terrestrial Ecosystem Model CTEM
160 (Arora and Boer, 2005). In this module, three aspects of the fire triangle are considered – the availability
161 of fuel to burn, the flammability of vegetation depending on environmental conditions, and the presence
162 of an ignition source. The natural ignition probability is summed to arbitrary anthropogenic fire
163 probability, and the burned area is modeled as an ellipse of dimensions determined by wind and fuel
164 conditions (Arora and Boer, 2005).

165 2.3 Observed data

166 2.3.1 Phosphorus databases

167 We used two P databases to estimate V_{\max} (Equation 1): one regional (referred to as PR) and one
168 global database referred to as PG). In addition, a control P map (PC) represents the unlimited nutrient
169 availability case, equivalent to a V_{\max} of $65 \mu\text{molCO}_2 \text{ m}^{-2} \text{ s}^{-1}$, or 350 mg P kg^{-1} soil, according to Equation
170 1.

171 The PR database was developed from total P in the soil for the Amazon basin published by
172 Quesada et al. (2011) plus 54 additional available P samples (P extracted via Mehlich-1 extractor,
173 $P_{\text{mehlich-1}}$) (Figure 2a). We used the $P_{\text{mehlich-1}}$ and clay contents measured in a forest-savanna transition
174 region in Brazil (Mato Grosso state) to estimate P_{total} and expand the coverage area of the P data (Section
175 S1). These 54 samples were gridded to a $1^\circ \times 1^\circ$ grid to be compatible with the spatial resolution used by
176 INLAND, resulting in 12 additional pixels with observed total P content (Figure 2a). For pixels without
177 observed P_{total} , the P_{total} was assumed to be 350 mg P kg^{-1} soil, similarly to the PC conditions.



178 A global dataset of P_{total} (Figure 2b) was also used to estimate V_{max} . This global data set is part of
179 a database containing six global maps of the different forms of P in the soil (Yang et al., 2013). The P_{total}
180 was estimated from lithologic maps, distribution of soil development stages, fraction of the remaining
181 source material for different stages of weathering using chronosequence studies (29 studies), and P
182 distribution in different forms for each soil type based on the analysis of Hedley fractionation (Yang and
183 Post, 2011), which are part of a worldwide collection of soil profile data. The uncertainties and limitations
184 associated with this database are restricted to the Hedley fractionation data used, which are 17% for low
185 weathered soils, 65% for intermediate soils and 68% for highly weathered soils (Yang et al., 2013).

186 2.3.2 Above-Ground AGB (AGB) database

187 The AGB database used was created by Nogueira et al. (2015) and considered undisturbed (pre-
188 deforestation) vegetation existing in the Brazilian Amazonia. This database was compiled from a
189 vegetation map at a scale of 1:250000 (IBGE, 1992) and AGB averages from 41 published studies that
190 had conducted direct sampling in either forest (2317 plots) or non-forest or contact zones (1830 plots).
191 We bi-linearly interpolated the AGB (dry weight) for each transect considering $1^\circ \times 1^\circ$ to ensure
192 compatibility of the observed and simulated data.

193 Five longitudinal transects (Figure 1) were used separately to characterize AGB in the Amazon-
194 Cerrado border (Figures 3a and 3b). In T1, T2, T3 and T4, the higher AGB values in the west and lower
195 values in the east are consistent with the transition from a dense and woody vegetation (the Amazon
196 forest) towards a sparse vegetation with lower AGB (the Cerrado). However, T1 shows a more gradual
197 reduction of AGB along the west to east gradient, while in T2, T3 and T4 where the transition is more



198 abrupt. In T5 no west-east gradient is present with high AGB heterogeneity and predominant low AGB
199 across the transect (Figure 3b).

200

201 **2.4 Simulations**

202 The model was forced with the prescribed climate data based on the Climate Research Unit (CRU)
203 database (Harris et al., 2014). Two climate boundary conditions were used: the first is referred to as the
204 monthly climatological average (CA) that represents the average climate for the period 1961-1990. The
205 second climate boundary condition is the historical dataset, for the continuous period between 1948 and
206 2008 (CV). For both boundary conditions, the variables used are rainfall, solar radiation, wind velocity
207 and maximum and minimum temperatures. The CRU database has been widely used by the scientific
208 community in case studies, because these data preserve the spatial mean of the rainfall data, although,
209 they do not provide adequate representation of their variance precipitation (Beguería et al., 2016). The
210 dataset has a 1-degree spatial resolution and a monthly time resolution.

211 Soil texture data is based on the IGBP-DIS global soil (Global Soil Data Task 2000) (Hansen and
212 Reed, 2000). The model simulations were run for the time period 1582-2008, a total of 427 years. In the
213 CV group of runs, the model was spin-up by cycling the 1948-2008 climate data (61-year) seven times,
214 totaling 427 years. In the CA group of runs, the annual mean climate data was cycled 427 times. In both
215 cases, CO₂ varied from 278 to 380 ppmv, according to observations in the period, updated annually. In
216 both cases, only the model results of the last 10 years were used to analyze the results.

217 The experiment design is a factorial combination of the climate scenarios (CA, monthly
218 climatological average, 1961-1990; CV, monthly climate time series, 1948-2008), the nutrient limitation



219 on V_{\max} (PC, no P limitation ($V_{\max} = 65 \mu\text{molCO}_2 \text{ m}^{-2} \text{ s}^{-1}$); PR, regional P limitation; PG, global P
220 limitation) and the occurrence of fire (F) or not (Table 1). The 12 combinations in Table 1 allow the
221 evaluation of individual and combined effects of climate, soil chemistry, and the incidence of fire on the
222 variables: Net Primary Production (NPP), tree AGB, and LAI of the upper and lower canopies ($\text{LAI}_{\text{upper}}$,
223 $\text{LAI}_{\text{lower}}$).

224 We consider that the subtraction between the simulations $(\text{CV}+\text{PC}) - (\text{CA}+\text{PC}) = (\text{CV}-\text{CA})|_{\text{PC}}$
225 represents the isolated effect of inter-annual climate variability without P limitations. The same logic is
226 applied to isolate other factors such as fire and P in different climate scenarios. For example, the fire
227 effect under average climate without P limitation case is calculated by the difference between $\text{CA}+\text{PC}+\text{F}$
228 and $\text{CA}+\text{PC}$, so that $(\text{CA}+\text{PC}+\text{F}) - (\text{CA}+\text{PC}) = \text{F}|_{\text{CA,PC}}$. Similarly, the isolated effect of fire under a climate
229 with inter-annual variability scenario without influence of P limitation is calculated by the difference
230 between $\text{CV}+\text{PC}+\text{F}$ and $\text{CV}+\text{PC}$, so that $(\text{CV}+\text{PC}+\text{F}) - (\text{CV}+\text{PC}) = \text{F}|_{\text{CV,PC}}$. The different combinations of
231 climate scenarios with and without fire effects and with and without P limitations are described in Table
232 2.

233 2.5 Statistical analysis and determination of the best model configuration

234 The statistical analysis is divided in four parts. First, we present maps of the isolated effects for
235 all simulated area calculated as the average of last ten years of simulated spatial patterns. The statistical
236 significance of the isolated effects on NPP, LAI and AGB are determined using the t-test with $p < 0.05$.
237 The results are tested in each pixel, for all the simulated domain ($n = 10$).

238 Second, we present an analysis of variance using the one-way ANOVA and the Tukey-Kramer
239 test in the transition zone. We consider all 31 pixels which fall in transects T1 to T5 (n_{pixels}). The results



240 presented are based on the set of last 10 years of simulation (1999-2008, n_{years}) for the 12 combinations
241 ($n_{\text{simulation}}$) in Table 1. Moreover, we grouped treatments according to climate regardless of P limitation,
242 presence or absence of fire, where all sets with CV vs CA are tested (Group 1, $n=1860$, ($n_{\text{pixel}} \times n_{\text{year}} \times$
243 ($n_{\text{simulation}}/2$)). Similarly, in Group 2 we tested if PC, PR or PG were significantly different from each other
244 regardless the F or climate used (Group 2, $n=1240$, ($n_{\text{pixel}} \times n_{\text{year}} \times (n_{\text{simulation}}/3)$). In Group 3 we tested if
245 fire introduced a significant effect regardless of climate and P limitation (Group 3, $n=1860$, ($n_{\text{pixel}} \times n_{\text{year}}$
246 $\times (n_{\text{simulation}}/2)$). Finally, all treatments were tested to each simulation assessing their individual effects on
247 NPP, LAI and AGB ($n_{\text{pixel}} \times n_{\text{year}} = 310$).

248 Third, a correlation coefficient between the simulated and observed values for AGB was
249 calculated for each transect. The simulated variables are averaged for the last 10 years of simulations
250 (1999 - 2008) and compared to AGB from Nogueira et al. (2015) within a grid cell.

251 Finally, we evaluate INLAND's ability to assign the dominant vegetation type by analyzing 10
252 years of probability of occurrence. If the dominant vegetation type (evergreen tropical forest, or deciduous
253 forest for the Amazon rainforest, and savanna or grasslands for Cerrado) in a pixel is the same in more
254 than 90% of the simulated years (9 out of 10), then the simulated vegetation type is defined as "very
255 robust" for that pixel; if it occurs in 70 - 90% of the simulated years, the simulated result is considered to
256 be "robust". If the dominant vegetation occurred in less than 70% of simulated years, the pixel is
257 considered "transitional" vegetation.



258 3 Results

259 3.1 Influence of climate, fire and phosphorus in the Amazon-Cerrado transition region

260 3.1.1 Spatial patterns

261 Overall, the inclusion of inter-annual climate variability (CV) resulted in a decrease in the
262 simulated average tree biomass (TB) by 3.8% in Amazonia, and by 8.7% in Cerrado in comparison to
263 average climate (CA) (Figure 4a). The spatial differences between CV and CA for TB simulations are
264 statistically significant and range from -3 kg-C m^{-2} to $+2 \text{ kg-C m}^{-2}$. The state of Pará, with higher
265 influence of the El Niño phenomenon, experienced the highest decrease in TB in the CV simulation. In
266 the state of Roraima, on the other hand, there was an increase of about 2 kg-C m^{-2} in TB when CV was
267 considered. Bolivia and southwest of Mato Grosso state also presented, in some grids points, a significant
268 increase in AGB higher than 2 kg-C m^{-2} .

269 On average, P acts as a limiting factor in the simulated TB, decreasing by 13% in regional P (PR)
270 simulation and 15% in global P (PG) simulation. In PR, TB decreased mainly in the southeastern
271 Amazonia (between Pará and northeastern Mato Grosso states) and northwestern Amazonas state (Figure
272 4b). In PG, the largest TB decline occurred in central Amazonia, northeastern Pará and northeastern Mato
273 Grosso (Figure 4c). In Cerrado, on the other hand, TB declined by 2% for PR and 9% for PG with respect
274 to the control simulation. In PR, the few pixels in the Cerrado that have P limitation showed a significant
275 decrease in TB (Figure 4b), while in PG the TB reduction was statistically significant for most of the
276 Cerrado domain, except in southern Tocantins state (Figure 4c).

277 The tree biomass reduction due to fire events is much higher in magnitude more than due to P
278 limitation or inter-annual climate variability (Figure 4d). The greater water availability is related to small



279 or null fire effect in the Central Amazon rainforest agrees with the fact that Amazonia is naturally
280 inflammable as well as a gradient towards seasonally dryer climate that increases the intensity and
281 magnitude of fire effects towards the Cerrado (Figure 4d). The fire effect on TB over the Amazon domain
282 was 21-24% of the P limitation effect (range for PR and PG cases), while the fire effect on TB over the
283 Cerrado was more than 250% of the P limitation effects in CV simulations, which is due to quick growth
284 of grasses after fire occurrence in the latter.

285 **3.1.2 Influence of climate, fire and phosphorus in the transects**

286 Results of the ANOVAs and Tukey-Kramer test indicate that the inclusion of CV, limitation by P
287 (PR and PG) and fire in INLAND led to significantly different averages of NPP, LAI and AGB in the
288 transition zones. This influence of climate, P and fire are shown separately in Tables 3 to Table 5 and
289 combined in Table 6.

290 The effects of climate and P on productivity show that CV reduces the NPP from
291 $0.68 \text{ kg-C m}^{-2} \text{ yr}^{-1}$ to $0.64 \text{ kg-C m}^{-2} \text{ yr}^{-1}$ (Table 3) and the P effect results in NPP decline from
292 $0.71 \text{ kg-C m}^{-2} \text{ yr}^{-1}$ to $0.64 \text{ kg-C m}^{-2} \text{ yr}^{-1}$ (both PR and PG) (Table 4). The fire effect, moreover, has a
293 positive effect on NPP from $0.66 \text{ kg-C m}^{-2} \text{ yr}^{-1}$ when fire is off to $0.67 \text{ kg-C m}^{-2} \text{ yr}^{-1}$ when fires is on. This
294 difference, albeit low, is statistically significant (Table 5).

295 In addition CV and P limitation reduce the $\text{LAI}_{\text{total}}$ in the canopy (Table 3 and Table 4), increasing
296 three times $\text{LAI}_{\text{lower}}$ and decreasing $\text{LAI}_{\text{upper}}$ (Table 5). The magnitude of fire effect on AGB (46.7%,
297 Table 5) is greater in relation to the CV (5%, Table 3) and P (14%, Table 4) limitation effects.

298 Even though CV effects on NPP and AGB for each simulation is not statistically significant, the
299 effects of fire and P limitation (regardless of phosphorus map) are. Fire effects are significant only for



300 structural variables as AGB, LAI_{total} , LAI_{upper} and LAI_{lower} . It presents an increase of LAI total of
301 $1.52 \text{ m}^2 \text{ m}^{-2}$ in CV+PG+F in relation to CV+PG, and of $1.32 \text{ m}^2 \text{ m}^{-2}$ in CV+PR+F in relation to CV+PR
302 (Table 6).

303 **3.1.3 West-East patterns of AGB in the Amazon-Cerrado transition**

304 The model used in this study simulates > 80% of the observed AGB variability in all treatments
305 along the transition area except in T5 (Table 7). It shows that the model is able to capture AGB variability
306 along the transition area, which is relevant when compared to studies that simulate 50% of the observed
307 AGB variability (Senna et al., 2009; Castanho et al., 2013).

308 It is not possible to identify a treatment that best represents AGB in all transects (Table 7). A
309 combined analysis of Table 7 and Figure 5 indicates a general agreement that observed AGB decreases
310 from W to E in T1 to T4, and this is well captured by several configurations of the model, with specific
311 differences among them. Overall, CA and PC configurations, being the least disturbed treatments, yield
312 higher AGB, while the introduction of CV, PG and F reduce the AGB. However, the simulated results
313 may be above or below the observed ones, which suggests that additional local factors are not included
314 in the model.

315 The curves of AGB (Figure 5) show the impact of CV, PG and F along the W-E transition. PG
316 has a high influence on the transition, decreasing the ABG especially in the western part of the transects,
317 where the Amazon vegetation is predominant. This feature is particularly simulated in T3 and T4, where
318 PG decrease the AGB by 2 kg-C m^{-2} in the west pixels of these transects (Figure 5). In T1, T2 and T5,
319 AGB decline is also higher with P limitation when compared to the curves limited only by CV. However,
320 in T1 model simulations tend to underestimate the highest and the lowest AGB extremes, and the absolute



321 values were always underestimated, despite the improvement in correlation with the inclusion of the fire
322 component (Table 7).

323 Fire, however in T2, T3 and T4, is responsible to approach the simulated AGB to the observed
324 AGB in the eastern pixels into Cerrado domain (Figure 5). In T5 these relations are similar, with climate
325 presenting less influence on AGB decrease than P, and fire appears mainly as a reducer factor.

326 3.2 Simulated composition of vegetation

327 Most of the pixels in CA show very robust simulations, with more than 90% of the same vegetation
328 cover in the simulated last 10 years (Figure 6a-c and 6g-i). A larger number of pixels with transitional
329 vegetation were simulated in CV (Figure 6d-f and 6j-l). An even higher variability in CV compared
330 to CA simulations was observed when we added the effects of P limitation and fire (Figure 6a and 6j-l).

331 The vegetation composition in all P limitation scenarios for CA simulations resulted in robust
332 simulations for nearly all pixels, except for the north of Cerrado domain (Figures 6a, 6b and 6c). The
333 CA+PC and CA+PR simulations had the same vegetation composition, while CA+PG replaced the
334 deciduous forest by evergreen forest in the central Cerrado region, around 8°S 46°W (Figures 6A, 6B and
335 6C). This behavior might be related to the higher P_{total} values in PG than PR and PC for the Cerrado region
336 (Figure S1). Cerrado was better represented in CV+PC, CV+PR and CV+PG than in the same CA
337 combinations (Figure 6). The occurrence of forested areas in central Cerrado decreased in CV
338 combinations, these being replaced by the savanna or grassland vegetation class.

339 When the effect of fire was added to CA simulations, the model simulated an increase in the
340 uncertainty on the vegetation cover classification in the Cerrado region. The effect of fire reduced the
341 presence of deciduous forest in central Cerrado biome as well as in CA+PC, and the vegetation was



342 replaced by evergreen forest and savanna in CA+PC+F (Figures 6G, 6H, 6I). In CV simulations, fire
343 effect results in the replacement of the deciduous and perennial forest by savanna and grasses in all central
344 Cerrado region (Figures 6J, 6K and 6L).

345 For all combinations used, transitional forest areas in the northern and southwestern Cerrado
346 biome are not adequately represented. With >90% of concordance, INLAND assigns the existence of
347 tropical evergreen forest rather than deciduous forest in some pixels in the north of the transition, and the
348 existence of tropical evergreen forest rather than savanna in the southwest, indicating difficulty to
349 simulate transitional vegetation in these regions.

350 **4 Discussion**

351 The inclusion of CV, PR and PG and fire in INLAND showed significant influences on the
352 simulated vegetation structure and dynamics in the Amazon-Cerrado border (Figure 4 and Table 6),
353 suggesting that these factors play key role on vegetation structure in the forest-savanna border and can
354 improve the simulated representation of the current contact zone between these biomes. This is broadly
355 consistent with the literature that investigated causes of savanna existence in the real world (Hoffmann et
356 al., 2012; Dantas et al., 2013; Lehmann et al., 2014). In this study, the spatial analysis and the Tukey-
357 Kramer test (TK) show a difference in magnitude among these factors in vegetation, with fire occurrence
358 and P limitation being stronger than inter-annual climate variability along the transects (Figure 4).

359 The spatial analysis showed that CV declines AGB predominantly in eastern Amazonia (Figure
360 4a). Climate of this region is intensely affected by El Niño–Southern Oscillation (ENSO), which could
361 reduce precipitation by 50%, placing the vegetation under intense water stress (Botta and Foley, 2002;
362 Foley et al. 2002; Marengo et al., 2004; Andreoli et al., 2013; Hilker et al., 2014). This reduction in



363 rainfall in dry years brings in direct changes in carbon flux (NPP) and stocks in leaves and wood, leading
364 to changes in vegetation structure. In addition to inter-annual changes in the rainfall, inter-annual
365 variability in other climate variables in CV also affect AGB, as average, maximum and minimum
366 temperature, as well as wind speed and specific humidity, and influence photosynthesis on the model both
367 directly (through Collatz and Farquhar equations) and indirectly (e.g. through evapotranspiration). Our
368 results showed significant differences for most part of the biomes, except central Amazonia (Figure 4a),
369 where CV and precipitation seasonality have been pointed as secondary effects on vegetation (Restrepo-
370 Coupe et al., 2013), since there is no shortage of water availability during the dry season.

371 Along the Cerrado, lower water availability in some years in CV affects tree biomass, although
372 that vegetation is predominantly grassy-herbaceous. The AGB decline is significant for most part of the
373 simulated Cerrado domain (Figure 4a) and average values could represent half the amount of typical tree
374 biomass in this biome. This reduction in AGB reflects INLAND's ability to simulate similar Cerrado
375 conditions and expose the few trees to high water stress.

376 Throughout the transects, however, no significant difference was found for average AGB between
377 CV+PC and CA+PC by TK at $p < 0.05$ (Table 6). On the other hand, when we analyzed the influence of
378 CV for the same pixels, but using all simulations (Table 3), regardless of P limitation and fire occurrences,
379 the results showed that the decrease in AGB by 0.38 kg-C m^{-2} (5.7%) is statistically significant along the
380 transition.

381 P limitation effect was statistically significant for PR and PG along all the Amazon domain and
382 the main differences between these simulations were the spatial patterns of tree AGB decrease (Figure 4b
383 and Figure 4c). We cannot affirm which of these databases is better because they are the results of



384 different methodologies and observations (Quesada et al., 2009; Yang et al., 2014). However, PG showed
385 a higher AGB decrease in central Amazonia, northeastern Pará and northeastern Mato Grosso state,
386 indicating that in these areas the P limitation is higher. This result does not corroborate the northwest-
387 southeast AGB gradient found in the Amazon basin, which showed a higher productivity in the west
388 where soils are more fertile than those found in the southeast (Aragão et al., 2009; Saatchi et al., 2007;
389 Nunes et al., 2012; Lee et al., 2013). On the other hand, PR AGB agrees with the northwest-southeast
390 gradient, presenting less limitation in the soils of central Amazonia with declines in AGB mainly in the
391 southeastern part of the rainforest (between Pará and northeastern Mato Grosso states) (Figure 4b).

392 In Cerrado, P limitation also influenced vegetation (Figure 4c) and presented statistically
393 significant differences when compared to CV+PC. In this biome, as well as in the Amazon, tree abundance
394 richness and diversity have been generally associated with increases of soil fertility (Long et al., 2012;
395 Vourtilis et al., 2013), highlighting the importance of P in the composition and maintenance of vegetation,
396 especially in transition areas.

397 Compared to the Amazon domain, the magnitude of effects of P limitation is lower in the Cerrado.
398 However, few pixels in PR that have P limitation showed a significant decrease in arboreal AGB (Figure
399 4b), while in PG, we found reduction of AGB for most of the Cerrado domain, except only for the southern
400 Tocantins state (Figure 4c). Despite the differences in spatial patterns, there was no statistically significant
401 differences between PR and PG within the transects (Table 4 and Table 6).

402 The spatial difference between PG and PR showed that PG is lower than PR in the western
403 Amazonia, and higher in northern Amazonia. Moreover, PG have low P values in south of the transition
404 compared to PR, while in Cerrado domain P values ranged between 120 to 200 mg kg⁻¹ (Figure S1).



405 Although the PR dataset includes every known P data collected in the region, these differences reinforce
406 the need to improve the data of P_{total} in the soils of the Amazon and Cerrado/Amazon transition domains.
407 Currently, P_{total} data in Cerrado is scarce, and make unfeasible to establish a proxy similar to Castanho et
408 al. (2013), which was specific for the Amazon.

409 To our knowledge, the most part of the Dynamic Global Vegetation Models (DGVMs) do not
410 consider the complete phosphorus cycle, despite the importance of nutrient cycling for AGB maintenance
411 and tropical vegetation dynamics in dystrophic soils. For example, nutrient cycling in the
412 Amazon/Cerrado transition is closely related to the hyper-dynamic turnover of the AGB (Valadão et al.
413 2016), in which some key species might also be crucial to the hyper-cycling of nutrients through which
414 vegetation sustain the constant input of nutrients, including large annual amounts of available P (Oliveira
415 et al. 2017).

416 The decrease in tree AGB occasioned by P limitation can contribute to a decrease in litter
417 production and consequently could affect nutrient cycling in tropical ecosystems. According to Oliveira
418 et al. (2017), the litter produced by vegetation corresponds to the main return route to the available fraction
419 of P for plants, especially in the transition areas, where $P_{\text{available}}$ in the soil is very low. In our model,
420 however, P acts directly in the photosynthesis limitation through V_{max} and cannot be reabsorbed by the
421 roots. Thus, the litter produced in vegetation contribute only to dry matter and fire occurrence increase.
422 In nature, the litter affected by fire occurrence volatilizes the small amount of P available to plants,
423 increasing the nutrient losses of the ecosystem. Despite this simplified representation in INLAND, it can
424 represent the P influence on woody AGB in the Amazon and Cerrado.



425 The fire occurrence is an important factor controlling the AGB dynamics in the Cerrado or in the
426 transition vegetation (Silvério et al., 2013; Couto-Santos et al., 2014; Balch et al., 2015), which this study
427 clearly replicates, showing statistically significant influences when compared to control simulations
428 (Figure 4d and Table 5). In the transition, the fire effect may reduce average AGB by 50%, which under
429 climate change or deforestation conditions may lead to an even stronger change in the vegetation structure
430 and dynamic. In the Cerrado domain, the simulated fire effect implies in significant increases of shrubs
431 and herbaceous vegetation and decreases of the arboreal component. In nature, however, the Cerrado is
432 relatively resilient to fire depending on the velocity, intensity and duration of the burning (Rezende et al.,
433 2005; Elias et al., 2013 Reis et al., 2015). The adaptive morphological nature and the low nutrient
434 requirement of vegetation allow Cerrado the capacity to rapidly restore the vegetation after fire occurrence
435 (Hoffmann et al., 2005; Hoffmann et al., 2012). In our model, the restoration of vegetation after fire
436 occurrence is exclusively due to the canopy opening and consequently more luminosity penetration into
437 lower canopy.

438 This study shows an improvement in the correlations between simulated and observed AGB when
439 compared to previous modeling studies, regardless of treatment, with correlation coefficients usually
440 above 0.80 for the transects, except for T5, for which the correlation coefficient value is usually below
441 0.5 (Table 7). Senna et al. (2009) found 0.20 as maximum correlation coefficient between simulated and
442 observed ABG while Castanho et al. (2013) showed 0.80 for Amazonia domain. From Figure 5, it is clear
443 that CV, F and P limitation in the transition zone reduce the AGB, approaching the simulated to the
444 observed data, and play important roles in the simulations, but the only inclusion of these effects is still
445 insufficient to represent the actual vegetation structure in the Amazon-Cerrado border (Figure 6L). In our



446 interpretation, this means that other important factors are still missing from the simulation, especially in
447 T5, where soils are rocky and shallow. A better spatial representation of soil physical properties, including
448 shallow rocky soils, as well as spatially varying physiological parameterizations of the vegetation such as
449 carbon allocation, deciduousness of vegetation, and residence time are probably needed to improve the
450 simulations, in particular in the northern and southern extremes of the border (T1 and T5).

451 In addition, literature shows that in the transition area, soils are very different than Amazon soils,
452 and that essential properties for modeling are peculiar (Silva et al., 2006; Vourlitis et al., 2013; Dias et
453 al. 2015). For example, Dias et al. (2015) recently showed that the pedological functions normally used
454 by DGVMs may underestimate the saturated hydraulic conductivity (K_s) by >99%, transforming a well-
455 drained soil with $K_s = 1.5 \cdot 10^{-4} \text{ m.s}^{-1}$ (540 mm.h^{-1}) in reality into an impervious brick with
456 $K_s = 3.3 \cdot 10^{-7} \text{ m.s}^{-1}$ (1.2 mm.h^{-1}) in the model.

457 For all transects, the AGB curves have similar patterns (Figure 5); the smaller difference is
458 observed between CA+PC and CV+PG curves, while the larger difference is when fire is present. The
459 effect of P limitation appears as an effect of intermediate magnitude, reducing the AGB by more than the
460 effect of inter-annual climate variability. In the east, it is observed that there is little or no difference
461 among AGB simulated by CA+PC, CV+PC and CV+PG, revealing that inter-annual climate variability
462 and P have smaller influence in the AGB. However, in the east of T2, T3 and T4, fire is the factor that
463 adjusts the simulated to the observed data (Figure 5), differently than the grid points in the West, where
464 CV+PG is a better proxy between observed and simulated data.

465 Such conditions are interesting because they reflect the different mechanisms that regulate the
466 structure of these ecosystems and probably the phytophysionomies distribution. For example, P



467 limitation seems to be the factor that improves simulated AGB in regions where the predominant
468 vegetation type is the tropical rainforest. Fire, on the other hand, improves the AGB in grid points where
469 the Cerrado occurs. Moreover, important factors such as productivity partitioning into leaves, roots and
470 wood carbon pools are assumed to be fixed in space and time within a given PFT, neglecting the natural
471 capacity of transitional forests to adapt itself and to adjust their metabolism to local environmental
472 conditions (Senna et al., 2009). In years of severe drought, transitional forests could prioritize the stock
473 of carbon to fine roots instead of the basal increment to maximize access to available water, or make
474 hydraulic redistribution to maintain the greenness and photosynthesis rates. Brando et al. (2008) found
475 high sensitivity in carbon allocation for eastern Amazon basin trees, which reduced wood production by
476 13-60% in response to an artificial drought. Although in INLAND soil moisture can reduce the
477 photosynthetic rates during the months of lower rainfall, it does not dynamically change the allocation
478 rates, exposing the PFTs in these areas to severe water stress and underestimating the AGB, such as in
479 the west of T1 (Figure 5a).

480 T2, T3 and T4, located in the central part of the Amazon-Cerrado transition, showed the highest
481 average correlations between observed and simulated data (Table 7). For these transects, INLAND seems
482 to be able to capture the high variability of AGB gradient.

483 At T5, located at the south of the transition, the average correlations were low for all treatments,
484 indicating that INLAND has difficulty to represent the AGB gradient there (Table 7). However, it captures
485 the lower AGB as compared to the northern ones. In this region, the vegetation is characterized by a wide
486 diversity of physiognomies, which varies with other preponderant factors, such as lithology, soil depth,
487 topography and fertility. The observed data also showed high AGB variability, indicating that there are



488 changes in the vegetation structure, featuring medium-sized and small vegetation types on different soil
489 types. In INLAND, however, features such as lithology and water-table depth are not considered due to
490 the complexity of its representation on the large scale, limiting the representation of a heterogeneous
491 environment throughout the transition.

492 Different patterns of vegetation distribution along the Amazon-Cerrado border exist and are
493 influenced not only by inter-annual climate variability, P limitation, and fire, but also by the
494 ecophysiological parameters, which may have different behavior according to the environmental
495 conditions and soil properties. Obtaining these parameters is a challenge to the scientific community
496 once the field measurements are difficult due to the extension of the transition area. More observed data
497 are needed to establish and implement the plasticity of the fixed parameters such as carbon coefficients
498 allocation, residence time, dependence of the deciduousness on P, among others.

499 Another point to discuss is that the model simulates, in a few pixels in southeastern Cerrado, very
500 robust simulations of the presence of savanna and grassland even in the absence of fire (Figure 6A-F and
501 6a-f). This is, in our view, a result of the intense water and heat stress in this region. In the Brazilian
502 Cerrado, the high temperatures ($> 35\text{ }^{\circ}\text{C}$) combined to the dry season duration (as long as 6 months with
503 little or no rain) exposes the vegetation to a severely stressed situation, so that a low biomass, low LAI
504 vegetation may exist without the need of a frequent disturbance.

505

506 **5 Conclusions**

507 This is the first study that uses modeling to assess the influence of inter-annual climate variability,
508 fire occurrence and phosphorus limitation to represent the Amazon-Cerrado border. This study shows



509 that, although the model forced by a climatological database is able to simulate basic characteristics of
510 the Amazon-Cerrado transition, the addition of factors such as inter-annual climate variability,
511 phosphorus limitation and fire gradually improves simulated vegetation types. These effects are not
512 homogeneous along the latitudinal/longitudinal gradient, which makes the adequate simulation of
513 biomass challenging in some places along the transition. Our work shows that fire is in the main
514 determinant factor of the vegetation changes along the transition. The nutrient limitation is second in
515 magnitude, stronger than the effect of inter-annual climate variability.

516 Overall, although INLAND typically simulates more than 80% of the variability of biomass in the
517 transition zone, in many places the biomass is clearly not well simulated. Situations for clearly wet or
518 markedly dry climate conditions were well simulated, but the simulations are generally poor for
519 transitional areas where the environment selected physiognomies that have an intermediate behavior, as
520 is the case of the transitional forests in northern Tocantins and Mato Grosso.

521 The lack of field parameters measured in the transition zone is still a major limitation to improve
522 the DGVMs. Spatially explicit carbon allocation strategies, mortality rates, physiological and structural
523 parameters are necessary to establish numerical relationships between the environment and the vegetation
524 dynamic models to make them able to correctly simulate current patterns and future changes in vegetation
525 considering future climate change. In addition, it is also needed to include not only the spatial variability,
526 but also temporal variability in physiological parameters of vegetation, allowing a more realistic
527 simulation of the vegetation-climate relationship. Finally, our results reinforce the importance and need
528 of the DGVMs to incorporate the nutrient limitation and fire occurrence to simulate the actual Amazon-
529 Cerrado border position.



530

531 **6 Acknowledgements**

532 We gratefully thank FAPEMIG and CAPES (Brazil) for their financial support. Atul K Jain is
533 funded by the U.S. National Science Foundation (NSF-AGS- 12-43071).

534 **7 References**

535 Aragão, L. E. O. C., Malhi, Y., Metcalfe, D. B., Silva-Espejo, J. E., Jiménez, E., Navarrete, D.,
536 Almeida, S., Costa, A. C. L., Salinas, N., Phillips, O. L., Anderson, L. O., Baker, T. R., Goncalvez, P. H.,
537 Huamán-Ovalle, J., Mamani-Solórzano, M., Meir, P., Monteagudo, A., Peñuela, M. C., Prieto, A.,
538 Quesada, C. A., Rozas-Dávila, A., Rudas, A., Silva Junior, J. A. and Vásquez, R.: Above- and below-
539 ground net primary productivity across ten Amazonian forests on contrasting soils, *Biogeosciences*, 6,
540 2441–2488, doi:10.5194/bgd-6-2441-2009, 2009.

541 Arora, V. K. and Boer, G. J.: A parameterization of leaf phenology for the terrestrial ecosystem
542 component of climate models, *Glob. Chang. Biol.*, 11, 39–59, doi:10.1111/j.1365-2486.2004.00890.x,
543 2005.

544 Balch, J. K., Brando, P. M., Nepstad, D. C., Coe, M. T., Silvério, D., Massad, T. J., Davidson, E.
545 A., Lefebvre, P., Oliveira-Santos, C., Rocha, W., Cury, R. T. S., Parsons, A. and Carvalho, K. S.: The
546 Susceptibility of Southeastern Amazon Forests to Fire: Insights from a Large-Scale Burn Experiment,
547 *Bioscience*, 65(9), 893–905, doi:10.1093/biosci/biv106, 2015.

548 Baudena, M., Dekker, S. C., Van Bodegom, P. M., Cuesta, B., Higgins, S. I., Lehsten, V., Reick,
549 C. H., Rietkerk, M., Scheiter, S., Yin, Z., Zavala, M. A. and Brovkin, V.: Forests, savannas, and



550 grasslands: Bridging the knowledge gap between ecology and Dynamic Global Vegetation Models,
551 Biogeosciences, 12(6), 1833–1848, doi:10.5194/bg-12-1833-2015, 2015.

552 Beguería, S., Vicente-Serrano, S. M., Tomás-Burguera, M. and Maneta, M.: Bias in the variance
553 of gridded data sets leads to misleading conclusions about changes in climate variability. *Int. J. Climatol.*,
554 36: 3413–3422. doi:10.1002/joc.4561, 2016.

555 Betts, R. A., Cox, P. M., Collins, M., Harris, P. P., Huntingford, C. and Jones, C. D.: The role of
556 ecosystem-atmosphere interactions in simulated Amazonian precipitation decrease and forest dieback
557 under global climate warming, *Theor. Appl. Climatol.*, 78, 157–175, doi:10.1007/s00704-004-0050-y,
558 2004.

559 Bonan, G. B.: Forests and climate change: forcings, feedbacks, and the climate benefits of forests,
560 *Science*, 320(5882), 1444–1449, doi:10.1126/science.1155121, 2008.

561 Botta, A. and Foley, J. A.: Effects of climate variability and disturbances on the Amazonian
562 terrestrial ecosystems dynamics, *Global Biogeochem. Cycles*, 16(4), doi:10.1029/2000GB001338, 2002.

563 Brando, P. M., Nepstad, D. C., Davidson, E. A., Trumbore, S. E., Ray, D. and Camargo, P.:
564 Drought effects on litterfall, wood production and belowground carbon cycling in an Amazon forest:
565 results of a throughfall reduction experiment, *Philos. Trans. R. Soc. Lond. B. Biol. Sci.*, 363(1498), 1839–
566 48, doi:10.1098/rstb.2007.0031, 2008.

567 Castanho, A. D. A., Coe, M. T., Costa, M. H., Malhi, Y., Galbraith, D. and Quesada, C. A.:
568 Improving simulated Amazon forest AGB and productivity by including spatial variation in biophysical
569 parameters, *Biogeosciences*, 10(4), 2255–2272, doi:10.5194/bg-10-2255-2013, 2013.



- 570 Couto-Santos, F. R., Luizão, F. J. and Carneiro Filho, A.: The influence of the conservation status
571 and changes in the rainfall regime on forest-savanna mosaic dynamics in Northern Brazilian Amazonia,
572 *Acta Amaz.*, 44(2), 197–206, 2014.
- 573 Cox, P. M., Betts, R. A., Jones, C. D., Spall, S. A. and Totterdell, I. J.: Acceleration of global
574 warming due to carbon-cycle feedbacks in a coupled climate model, *Nature*, 408(November), 184–187,
575 doi:10.1038/35041539, 2000.
- 576 Cox, P. M., Betts, R. A., Collins, M., Harris, P. P., Huntingford, C. and Jones, C. D.: Amazonian
577 forest dieback under climate-carbon cycle projections for the 21st century, *Theor. Appl. Climatol.*, 78,
578 137–156, doi:10.1007/s00704-004-0049-4, 2004.
- 579 Dajoz, R.: *Princípios de ecologia*, 7^o edição, Artmed, Porto Alegre, RS, Brazil 519pp, 2005.
- 580 Dantas, V. L., Batalha, M. A. and Pausas, J. G.: Fire drives functional thresholds on the savanna-
581 forest transition, *Ecology*, 94(11), 2454–2463, doi:10.1890/12-1629.1, 2013.
- 582 Dias, L. C. P., Macedo, M. N., Costa, M. H., Coe, M. T. and Neill, C.: Effects of land cover change
583 on evapotranspiration and streamflow of small catchments in the Upper Xingu River Basin, Central
584 Brazil, *J. Hydrol. Reg. Stud.*, 4, 108–122, doi:10.1016/j.ejrh.2015.05.010, 2015.
- 585 Elias, F., Marimon, B. S., Matias, S. R. A., Forsthofer, M., Morandi, P. S. and Marimon-junior,
586 B. H.: Dinâmica da distribuição espacial de populações arbóreas, ao longo de uma década, em cerrado
587 na transição Cerrado-Amazônia, *Mato Grosso, Biota Amaz.*, 3, 1–14, 2013.
- 588 Favier, C., Chave, J., Fabing, A., Schwartz, D. and Dubois, M. A.: Modelling forest-savanna
589 mosaic dynamics in man-influenced environments: Effects of fire, climate and soil heterogeneity, *Ecol.*
590 *Modell.*, 171, 85–102, doi:10.1016/j.ecolmodel.2003.07.003, 2004.



591 Foley, J. A., Prentice, I. C., Ramankutty, N., Levis, S., Pollard, D., Sitch, S. and Haxeltine, A.: An
592 integrated biosphere model of land surface processes, terrestrial carbon balance, and vegetation dynamics,
593 Global Biogeochem. Cycles, 10, 603, doi:10.1029/96GB02692, 1996.

594 Foley, J. A., Botta, A., Coe, M. T. and Costa, M. H.: El Niño–Southern oscillation and the
595 climate, ecosystems and rivers of Amazonia, Global Biogeochem. Cycles, 16(4), 1132,
596 doi:10.1029/2002GB001872, 2002.

597 Goedert, W.: Solos do Cerrado: Tecnologias e Estratégias de Manejo, Empresa Brasileira de
598 Pesquisa Agropecuária (EMBRAPA), Brasília, DF, Brasil. 422pp., 1986.

599 Hansen, M. C. and Reed, B.: A comparison of the IGBP DISCover and University of Maryland
600 1km global land cover products, Int. J. Remote Sens., 21, 1365–1373, doi:10.1080/014311600210218,
601 2000.

602 Harris, I., Jones, P. D., Osborn, T. J. and Lister, D. H.: Updated high-resolution grids of monthly
603 climatic observations - the CRU TS3.10 Dataset, Int. J. Climatol., 34(3), 623–642, doi:10.1002/joc.3711,
604 2014.

605 Hirota, M., Nobre, C., Oyama, M. D. and Bustamante, M. M. C.: The climatic sensitivity of the
606 forest, savanna and forest-savanna transition in tropical South America, New Phytol., 187, 707–719,
607 doi:10.1111/j.1469-8137.2010.03352.x, 2010.

608 Hoffmann, W. A., Da Silva, E. R., Machado, G. C., Bucci, S. J., Scholz, F. G., Goldstein, G. and
609 Meinzer, F. C.: Seasonal leaf dynamics across a tree density gradient in a Brazilian savanna, Oecologia,
610 145, 307–316, doi:10.1007/s00442-005-0129-x, 2005.



- 611 Hoffmann, W. A., Geiger, E. L., Gotsch, S. G., Rossatto, D. R., Silva, L. C. R., Lau, O. L.,
612 Haridasan, M. and Franco, A. C.: Ecological thresholds at the savanna-forest boundary: How plant traits,
613 resources and fire govern the distribution of tropical biomes, *Ecol. Lett.*, 15, 759–768,
614 doi:10.1111/j.1461-0248.2012.01789.x, 2012.
- 615 House, J. I., Archer, S., Breshears, D. D. and Scholes, R. J.: Conundrums in mixed woody-
616 herbaceous plant systems, *J. Biogeogr.*, 30, 1763–1777, doi:10.1046/j.1365-2699.2003.00873.x, 2003.
- 617 IBGE.: Manual Técnico da Vegetação Brasileira (Manuais Técnicos em Geociências n. 1),
618 Fundação Instituto Brasileiro de Geografia e Estatística (IBGE), Rio de Janeiro, RJ, Brasil. 92pp., 1992.
- 619 IBGE.: Mapa da Vegetação do Brasil, Fundação Instituto Brasileiro de Geografia e Estatística
620 (IBGE), Rio de Janeiro, RJ, Brazil, Map, 2004.
- 621 Klink, C. A. and Machado, R. B.: Conservation of the Brazilian Cerrado, *Conserv. Biol.*, 19(3),
622 707–713, doi:10.1111/j.1523-1739.2005.00702.x, 2005.
- 623 Kucharik, C. J., Foley, J. A., Delire, C., Fisher, V. A., Coe, M. T., Lenters, J. D., Young-Molling,
624 C., Ramankutty, N., Norman, J. M. and Gower, S. T.: Testing the performance of a Dynamic Global
625 Ecosystem Model: Water balance, carbon balance, and vegetation structure, *Global Biogeochem. Cycles*,
626 14(3), 795–825, doi:10.1029/1999GB001138, 2000.
- 627 Lee, J. E., Frankenberg, C., van der Tol, C., Berry, J. A., Guanter, L., Boyce, C. K., Fisher, J. B.,
628 Morrow, E., Worden, J. R., Asefi, S., Badgley, G. and Saatchi, S.: Forest productivity and water stress in
629 Amazonia: observations from GOSAT chlorophyll fluorescence, *Proc. R. Soc. B Biol. Sci.*, 280(1761),
630 20130171–20130171, doi:10.1098/rspb.2013.0171, 2013.



631 Lehmann, C. E. R., Archibald, S. A., Hoffmann, W. A. and Bond, W. J.: Deciphering the
632 distribution of the savanna biome, *New Phytol.*, 191, 197–209, doi:10.1111/j.1469-8137.2011.03689.x,
633 2011.

634 Lehmann, C. E. R., Anderson, T. M., Sankaran, M., Higgins, S. I., Archibald, S., Hoffmann, W.
635 A., Hanan, N. P., Williams, R. J., Fensham, R. J., Felfili, J., Hutley, L. B., Ratnam, J., Jose, J. S., Montes,
636 R., Franklin, D., Russell-Smith, J., Ryan, C. M., Durigan, G., Hiernaux, P., Haidar, R., Bowman, D. M.
637 J. S., and Bond, W. J.: Savanna Vegetation-Fire-Climate Relationships Differ Among Continents,
638 *Science*, 343 (January), 548–553, doi:10.1126/science.1247355, 2014.

639 Long, W., Yang, X. and Donghai, L.: Patterns of species diversity and soil nutrients along a
640 chronosequence of vegetation recovery in Hainan Island, South China, *Ecol. Res.*, 2012.

641 Malhi, Y., Aragão, L. E. O. C., Metcalfe, D. B., Paiva, R., Quesada, C. A., Almeida, S., Anderson,
642 L., Brando, P., Chambers, J. Q., da Costa, A. C. L., Hutrya, L. R., Oliveira, P., Patiño, S., Pyle, E. H.,
643 Robertson, A. L. and Teixeira, L. M.: Comprehensive assessment of carbon productivity, allocation and
644 storage in three Amazonian forests, *Glob. Chang. Biol.*, 15, 1255–1274, doi:10.1111/j.1365-
645 2486.2008.01780.x, 2009.

646 Marimon Junior, B. H. and Haridasan, M.: Comparação da vegetação arbórea e características
647 edáficas de um cerradão e um cerrado sensu stricto em áreas adjacentes sobre solo distrófico no leste de
648 Mato Grosso, Brasil, *Acta Bot. Brasilica*, 19(4), 913–926, doi:10.1590/S0102-33062005000400026,
649 2005.



650 Marimon, B. S., Lima, E. S., Duarte, T. G., Chieregatto, L. C., Ratter, J. A.: Observations on the
651 vegetation of northeastern Mato Grosso, Brazil. IV. An analysis of the Cerrado-Amazonian Forest
652 ecotone, *Edinburgh Journal of Botany*, 63, 323–341, doi: 10.1017/S0960428606000576, 2006.

653 Marimon, B. S., Marimon-Junior, B. H., Feldpausch, T. R., Oliveira-Santos, C., Mews, H. A.,
654 Lopez-Gonzalez, G., Lloyd, J., Franczak, D. D., de Oliveira, E. A., Maracahipes, L., Miguel, A., Lenza,
655 E. and Phillips, O. L.: Disequilibrium and hyperdynamic tree turnover at the forest–cerrado transition
656 zone in southern Amazonia, *Plant Ecol. Divers.*, 7(1–2), 281–292, doi:10.1080/17550874.2013.818072,
657 2014.

658 Mercado, L. M., Patino, S., Domingues, T. F., Fyllas, N. M., Weedon, G. P., Sitch, S., Quesada,
659 C. A., Phillips, O. L., Aragao, L. E. O. C., Malhi, Y., Dolman, A. J., Restrepo-Coupe, N., Saleska, S. R.,
660 Baker, T. R., Almeida, S., Higuchi, N. and Lloyd, J.: Variations in Amazon forest productivity correlated
661 with foliar nutrients and modelled rates of photosynthetic carbon supply, *Philos. Trans. R. Soc. Lond. B.*
662 *Biol. Sci.*, 366(1582), 3316–3329, doi:10.1098/rstb.2011.0045, 2011.

663 Morandi, P.S., Marimon-Junior, B. H., Oliveira, E. A., Reis, S. M. A., Valadão, M. B. X.,
664 Forsthofer, M., Passos, F. B., Marimon, B. S.: Vegetation Succession in the Cerrado-Amazonian Forest
665 Transition Zone of Mato Gross State, Brazil, *Edinburgh Journal of Botany*, 73, 83-93, doi:
666 10.1017/S096042861500027X, 2016.

667 Moreno, M. I. C., Schiavini, I. and Haridasan, M.: Fatores edáficos influenciando na estrutura de
668 fitofisionomias do cerrado, *Caminhos da Geogr.*, 9(25), 173–194, 2008.

669 Murphy, B. P. and Bowman, D. M. J. S.: What controls the distribution of tropical forest and
670 savanna?, *Ecol. Lett.*, 15, 748–758, doi:10.1111/j.1461-0248.2012.01771.x, 2012.



- 671 Myers, N., Fonseca, G. A. B., Mittermeier, R. A., Fonseca, G. A. B. and Kent, J.: Biodiversity
672 hotspots for conservation priorities, *Nature*, 403(6772), 853–858, doi:10.1038/35002501, 2000.
- 673 Nardoto, G. B., Bustamante, M. M. C., Pinto, A. S. and Klink, C. A. Nutrient use efficiency at
674 ecosystem and species level in savanna areas of Central Brazil and impacts of fire, *J. Trop. Ecol.*, 22,
675 191–201, doi:10.1017/S0266467405002865, 2006.
- 676 Nogueira, E. M., Yanai, A. M., Fonseca, F. O. and Fearnside, P. M.: Carbon stock loss from
677 deforestation through 2013 in Brazilian Amazonia, *Glob. Chang. Biol.*, doi:10.1111/gcb.12798, 2015.
- 678 Nunes, E. L., Costa, M. H., Malhado, A. C. M., Dias, L. C. P., Vieira, S. A., Pinto, L. B. and Ladle,
679 R. J.: Monitoring carbon assimilation in South America's tropical forests: Model specification and
680 application to the Amazonian droughts of 2005 and 2010, *Remote Sens. Environ.*, 117, 449–463,
681 doi:10.1016/j.rse.2011.10.022, 2012.
- 682 Oliveira, B., Marimon-Junior, B. H., Mews, H. A., Valadão, M. B. X., Marimon, B. S.: Unraveling
683 the ecosystem functions in the Amazonia–Cerrado transition: evidence of hyperdynamic nutrient cycling,
684 *Plant Ecol.*, 218(2), 225–239, doi:10.1007/s11258-016-0681-y, 2017.
- 685 Oyama, M. D. and Nobre, C. A.: A new climate-vegetation equilibrium state for Tropical South
686 America, *Geophys. Res. Lett.*, 30(23), 10–13, doi:10.1029/2003GL018600, 2003.
- 687 Parton, W. J., Scurlock, J. M. O., Ojima, D. S., Gilmanov, T. G., Scholes, R. J., Schimel, D. S.,
688 Kirchner, T., Menaut, J.-C., Seastedt, T., Garcia Moya, E., Kamnalrut, A. and Kinyamario, J. I.:
689 Observations and modeling of AGB and soil organic matter dynamics for the grassland biome worldwide,
690 *Global Biogeochem. Cycles*, 7, 785, doi:10.1029/93GB02042, 1993.



691 Pereira, M. P. S., Malhado, A. C. M. and Costa, M. H.: Predicting land cover changes in the
692 Amazon rainforest: An ocean-atmosphere-biosphere problem, *Geophys. Res. Lett.*, 39(9),
693 doi:10.1029/2012GL051556, 2012.

694 Pires, G. F. and Costa, M. H.: Deforestation causes different subregional effects on the Amazon
695 bioclimatic equilibrium, *Geophys. Res. Lett.*, 40(14), 3618–3623, doi:10.1002/grl.50570, 2013.

696 Quesada, C. A., Lloyd, J., Schwarz, M., Baker, T. R., Phillips, O. L., Patiño, S., Czimczik, C.,
697 Hodnett, M. G., Herrera, R., Arneeth, A., Lloyd, G., Malhi, Y., Dezzee, N., Luizão, F. J., Santos, A. J. B.,
698 Schmerler, J., Arroyo, L., Silveira, M., Priante Filho, N., Jimenez, E. M., Paiva, R., Vieira, I., Neill, D.
699 A., Silva, N., Peñuela, M. C., Monteagudo, A., Vásquez, R., Prieto, A., Rudas, A., Almeida, S., Higuchi,
700 N., Lezama, A. T., López-González, G., Peacock, J., Fyllas, N. M., Alvarez Dávila, E., Erwin, T., di Fiore,
701 A., Chao, K. J., Honorio, E., Killeen, T., Peña Cruz, A., Pitman, N., Núñez Vargas, P., Salomão, R.,
702 Terborgh, J. and Ramírez, H.: Regional and large-scale patterns in Amazon forest structure and function
703 are mediated by variations in soil physical and chemical properties, *Biogeosciences Discuss.*, 6, 3993–
704 4057, doi:10.5194/bgd-6-3993-2009, 2009.

705 Quesada, C. A., Lloyd, J., Anderson, L. O., Fyllas, N. M., Schwarz, M. and Czimczik, C. I.: Soils
706 of Amazonia with particular reference to the RAINFOR sites, *Biogeosciences*, 8, 1415–1440,
707 doi:10.5194/bg-8-1415-2011, 2011.

708 Quesada, C. A., Phillips, O. L., Schwarz, M., Czimczik, C. I., Baker, T. R., Patiño, S., Fyllas, N.
709 M., Hodnett, M. G., Herrera, R., Almeida, S., Alvarez Dávila, E., Arneeth, A., Arroyo, L., Chao, K. J.,
710 Dezzee, N., Erwin, T., Di Fiore, A., Higuchi, N., Honorio Coronado, E., Jimenez, E. M., Killeen, T.,
711 Lezama, A. T., Lloyd, G., López-González, G., Luizão, F. J., Malhi, Y., Monteagudo, A., Neill, D. A.,



712 Núñez Vargas, P., Paiva, R., Peacock, J., Peñuela, M. C., Peña Cruz, A., Pitman, N., Priante Filho, N.,
713 Prieto, A., Ramírez, H., Rudas, A., Salomão, R., Santos, A. J. B., Schmerler, J., Silva, N., Silveira, M.,
714 Vásquez, R., Vieira, I., Terborgh, J. and Lloyd, J.: Basin-wide variations in Amazon forest structure and
715 function are mediated by both soils and climate, *Biogeosciences*, 9(6), 2203–2246, doi:10.5194/bg-9-
716 2203-2012, 2012.

717 Reis, S. M., Marimon, B. S., Marimon Junior, B.-H., Gomes, L., Morandi, P. S., Freire, E. G. and
718 Lenza, E.: Resilience of savanna forest after clear-cutting in the Cerrado-Amazon transition zone,
719 *Bioscience*, 31(5), 1519–1529, doi:10.14393/BJ-v31n5a2015-26368, 2015.

720 Restrepo-Coupe, N., da Rocha, H. R., Hutyra, L. R., da Araujo, A. C., Borma, L. S.,
721 Christoffersen, B., Cabral, O. M. R., de Camargo, P. B., Cardoso, F. L., da Costa, A. C. L., Fitzjarrald,
722 D. R., Goulden, M. L., Kruijt, B., Maia, J. M. F., Malhi, Y. S., Manzi, A. O., Miller, S. D., Nobre, A. D.,
723 von Randow, C., S, L. D. A., Sakai, R. K., Tota, J., Wofsy, S. C., Zanchi, F. B. and Saleska, S. R.: What
724 drives the seasonality of photosynthesis across the Amazon basin? A cross-site analysis of eddy flux tower
725 measurements from the Brazil flux network, *Agric. For. Meteorol.*, 182–183, 128–144,
726 doi:10.1016/j.agrformet.2013.04.031, 2013.

727 Rezende, A. V., Sanquetta, C. R. and Filho, F. A.: Efeito do desmatamento no estabelecimento de
728 espécies lenhosas em um cerrado *Sensu stricto*, *Floresta*, 35, 69–88, 2005.

729 Ribeiro, J. F. and Walter, B. M. T.: As Principais Fitofisionomias do bioma Cerrado, in *Cerrado:*
730 *ecologia e flora*, pp. 153–212., 2008.



- 731 Rocha, H. R. da, Goulden, M. L., Miller, S. D., Menton, M. C., Pinto, L. D. V. O., De Freitas, H.
732 C. and Figueira, A. M. E. S.: Seasonality of water and heat fluxes over a tropical forest in eastern
733 Amazonia, *Ecol. Appl.*, 14(4 SUPPL.), doi:10.1890/02-6001, 2004.
- 734 Roy, S. B. and Avissar, R.: Impact of land use/land cover change on regional hydrometeorology
735 in Amazonia, *J. Geophys. Res.*, 107(D20), 1–12, doi:10.1029/2000JD000266, 2002.
- 736 Ruggiero, P. G. C., Batalha, M. A., Pivello, V. R. and Meirelles, S. T.: Soil-vegetation
737 relationships in cerrado (Brazilian savanna) and semideciduous forest, Southeastern Brazil, *Plant Ecol.*,
738 160(1), 1–16, doi:10.1023/A:1015819219386, 2002.
- 739 Saatchi, S., Houghton, R. A., Dos Santos Alvalá, R. C., Soares, J. V. and Yu, Y.: Distribution of
740 aboveground live AGB in the Amazon basin, *Glob. Chang. Biol.*, 13(4), 816–837, doi:10.1111/j.1365-
741 2486.2007.01323.x, 2007.
- 742 Salazar, L. F., Nobre, C. A. and Oyama, M. D.: Climate change consequences on the biome
743 distribution in tropical South America, *Geophys. Res. Lett.*, 34(April), 2–7, doi:10.1029/2007GL029695,
744 2007.
- 745 Senna, M. C. A., Costa, M. H., Pinto, L. I.C., Imbuzeiro, H. M. A., Diniz, L. M. F. and Pires, G.
746 F.: Challenges to reproduce vegetation structure and dynamics in Amazonia using a coupled climate-
747 biosphere model, *Earth Interact.*, 13(11), doi:10.1175/2009EI281.1, 2009.
- 748 Shukla, J., Nobre, C. and Sellers, P.: Amazon deforestation and climate change, *Science*, 247,
749 1322–1325, doi:10.1126/science.247.4948.1322, 1990.
- 750 Silva, J. F., Fariñas, M. R., Felfili, J. M. and Klink, C. A.: Spatial heterogeneity, land use and
751 conservation in the cerrado region of Brazil, in *Journal of Biogeography*, vol. 33, pp. 536–548., 2006.



752 Silvério, D. V., Brando, P. M., Balch, J. K., Putz, F. E., Nepstad, D. C., Oliveira-Santos, C. and
753 Bustamante, M. M. C.: Testing the Amazon savannization hypothesis: fire effects on invasion of a
754 neotropical forest by native cerrado and exotic pasture grasses, *Philos. Trans. R. Soc. Lond. B. Biol. Sci.*,
755 368, 20120427, doi:10.1098/rstb.2012.0427, 2013.

756 Torello-Raventos, M., Feldpausch, T., Veenendaal, E., Schrod, F., Saiz, G., Domingues, T.,
757 Djagbletey, G., Ford, A., Kemp, J., Marimon, B., Hur Marimon Junior, B., Lenza, E., Ratter, J.,
758 Maracahipes, L., Sasaki, D., Sonké, B., Zapfack, L., Taedoumg, H., Villarroel, D., Schwarz, M., Quesada,
759 C., Yoko Ishida, F., Nardoto, G., Affum-Baffoe, K., Arroyo, L., Bowman, D., Compaore, H., Davies, K.,
760 Diallo, A., Fyllas, N., Gilpin, M., Hien, F., Johnson, M., Killeen, T., Metcalfe, D., Miranda, H., Steininger,
761 M., Thomson, J., Sykora, K., Mougín, E., Hiernaux, P., Bird, M., Grace, J., Lewis, S., Phillips, O. and
762 Lloyd, J.: On the delineation of tropical vegetation types with an emphasis on forest/savanna transitions,
763 *Plant Ecol. Divers.*, 6, 101–137, doi:10.1080/17550874.2012.76281, 2013.

764 Valadão, M. B. X., Marimon-Junior, B. H., Oliveira, B., Lúcio, N. W., Souza, M. G. R., Marimon,
765 B. S.: AGB hyperdynamic as a key modulator of forest self-maintenance in dystrophic soil at Amazonia-
766 Cerrado transition. *Scientia Forestalis*, 44, 475-485, 2016.

767 Veenendaal, E. M., Torello-Raventos, M., Feldpausch, T. R., Domingues, T. F., Gerard, F.,
768 Schrod, F., Saiz, G., Quesada, C. A., Djagbletey, G., Ford, A., Kemp, J., Marimon, B. S., Marimon-
769 Junior, B. H., Lenza, E., Ratter, J. A., Maracahipes, L., Sasaki, D., Sonk, B., Zapfack, L., Villarroel, D.,
770 Schwarz, M., Yoko Ishida, F., Gilpin, M., Nardoto, G. B., Affum-Baffoe, K., Arroyo, L., Bloomfield, K.,
771 Ceca, G., Compaore, H., Davies, K., Diallo, A., Fyllas, N. M., Gignoux, J., Hien, F., Johnson, M., Mougín,
772 E., Hiernaux, P., Killeen, T., Metcalfe, D., Miranda, H. S., Steininger, M., Sykora, K., Bird, M. I., Grace,



773 J., Lewis, S., Phillips, O. L. and Lloyd, J.: Structural, physiognomic and above-ground AGB variation in
774 savanna-forest transition zones on three continents - How different are co-occurring savanna and forest
775 formations?, *Biogeosciences*, 12(10), 2927–2951, doi:10.5194/bg-12-2927-2015, 2015.

776 Verberne, E. L. J., Hassink, J., De Willigen, P., Groot, J. J. R. and Van Veen, J. A.: Modelling
777 organic matter dynamics in different soils, *Netherlands J. Agric. Sci.*, 38, 221–238, 1990.

778 Vourlitis, G. L., de Lobo, F. A., Lawrence, S., de Lucena, I. C., Pinto, O. B., Dalmagro, H. J.,
779 Ortiz, C. E. and de Nogueira, J. S.: Variations in Stand Structure and Diversity along a Soil Fertility
780 Gradient in a Brazilian Savanna (Cerrado) in Southern Mato Grosso, *Soil Sci. Soc. Am. J.*, 77(4), 1370–
781 1379, doi:10.2136/sssaj2012.0336, 2013.

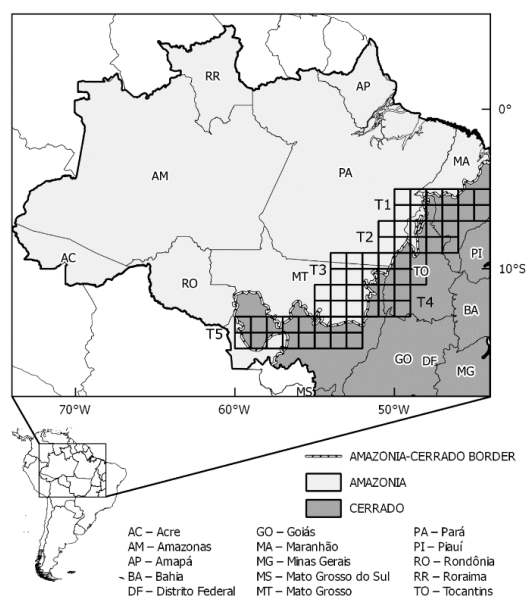
782 Yang, X. and Post, W. M.: Phosphorus transformations as a function of pedogenesis: A synthesis
783 of soil phosphorus data using Hedley fractionation method, *Biogeosciences*, 8, 2907–2916,
784 doi:10.5194/bg-8-2907-2011, 2011.

785 Yang, X., Post, W. M., Thornton, P. E. and Jain, A.: The distribution of soil phosphorus for global
786 biogeochemical modeling, *Biogeosciences*, 10, 2525–2537, doi:10.5194/bg-10-2525-2013, 2013.

787 Yang, X., Thornton, P. E., Ricciuto, D. M. and Post, W. M.: The role of phosphorus dynamics in
788 tropical forests - A modeling study using CLM-CNP, *Biogeosciences*, 11, 1667–1681, doi:10.5194/bg-
789 11-1667-2014, 2014.

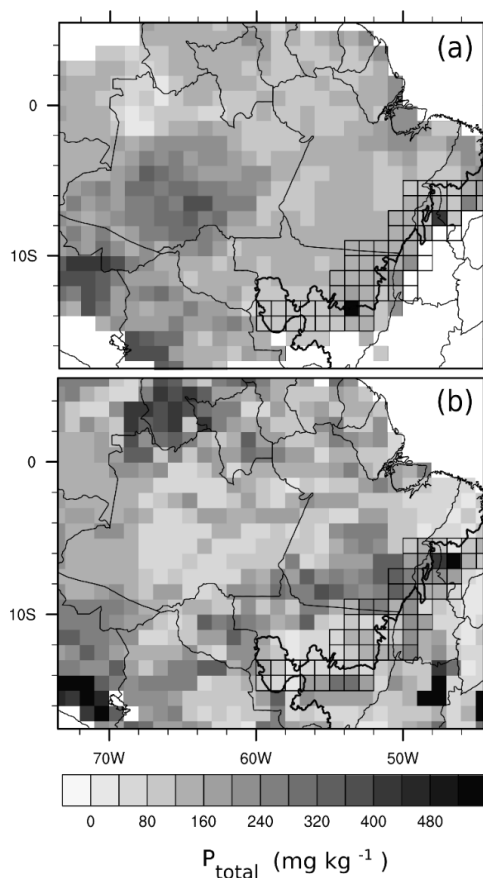
790

791



792

793 **Figure 1.** Delimitation of the study area Amazonia (in light gray) and Cerrado (in dark gray) (IBGE,
794 2004), and the location of five transects used in this work (from T1 to T5). The dashed line represents the
795 border between biomes.

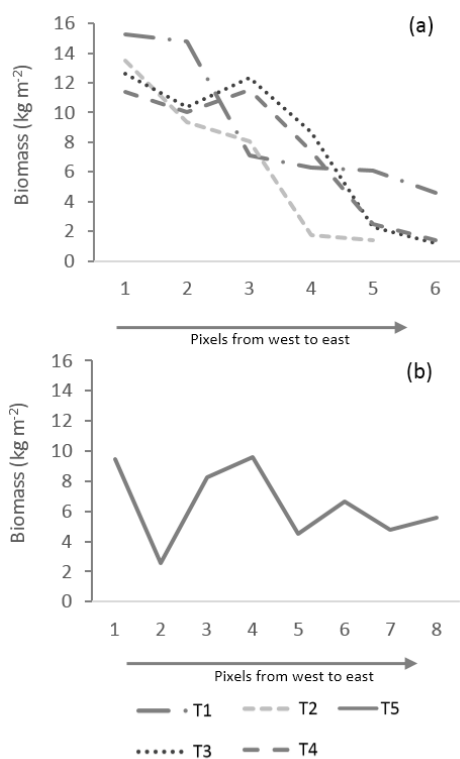


796

797 **Figure 2.** (a) Map of regional total P in the soil (PR), (b) Map of global total P in the soil (Yang et al.,

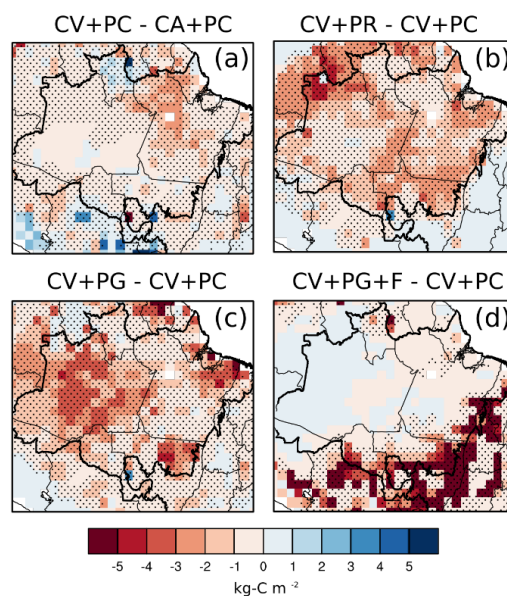
798 2013) (PG).

799



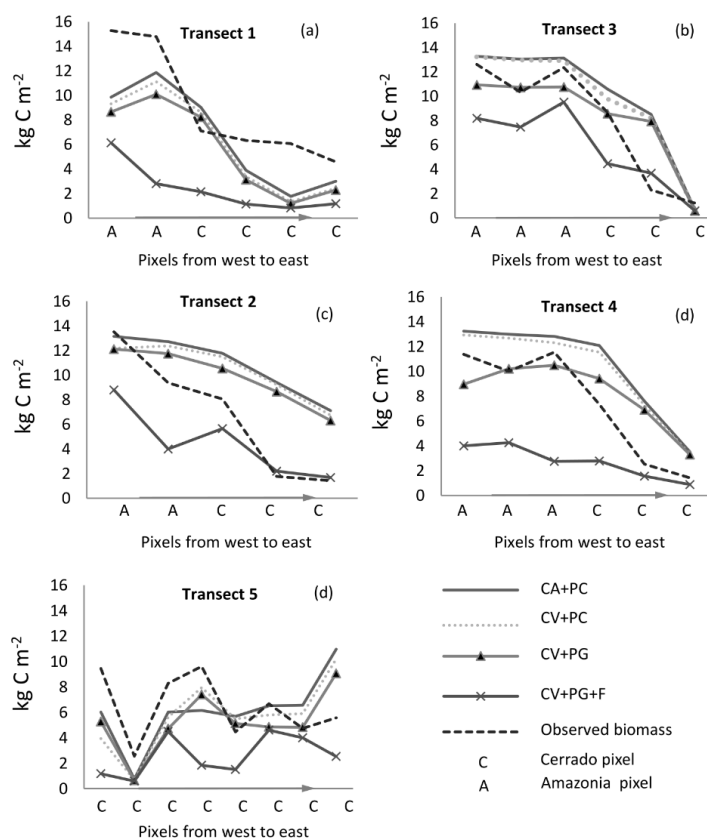
800

801 **Figure 3.** Variations of AGB in pixels from West to East in the Amazonia-Cerrado transition for
802 transects T1, T2, T3 and T4 (a), and T5 (b).



803

804 **Figure 4.** Effects of inter-annual climate variability (a), Regional P limitation (b), Global P limitation (c),
 805 and fire (d) on AGB. The hatched areas indicate that the variables are significantly different compared to
 806 the control simulation at the level of 95% according to the t-test. The thick black line is the geographical
 807 limits of the biomes.

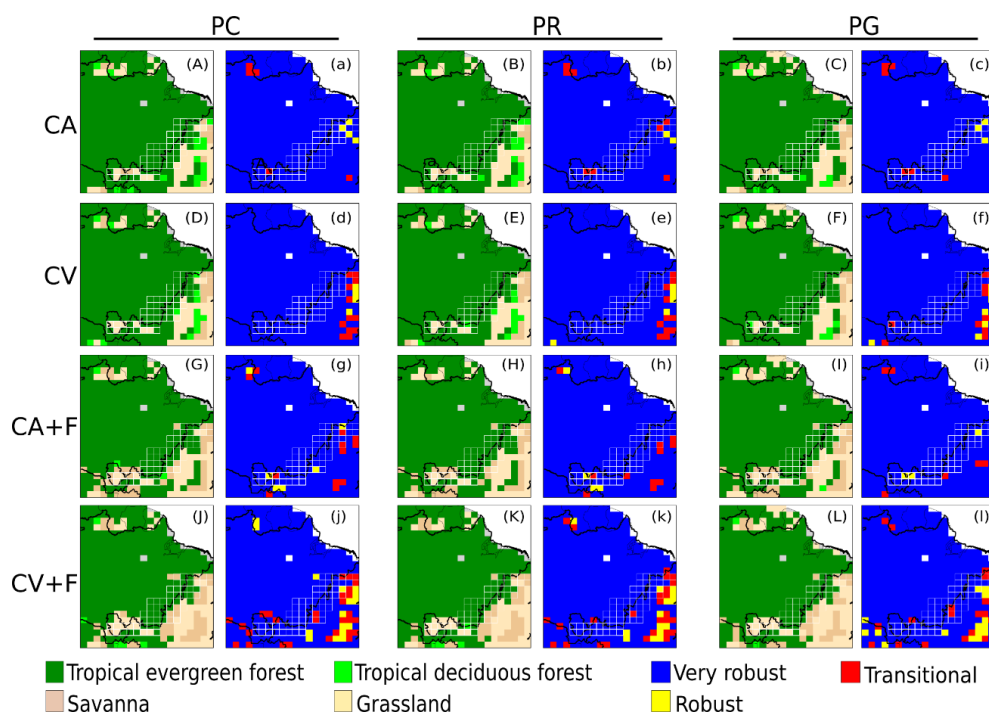


808

809 **Figure 5.** Longitudinal AGB gradient in Amazonia-Cerrado transition simulated for T1 to T5 considering
 810 different combinations: observed data; seasonal climate control simulation (CA+PC); inter-annual
 811 climate variability (CV+PC); inter-annual climate variability + global P limitation (CV+PG); and inter-
 812 annual climate variability + P + fire occurrence (CV+PG+F).



813



814

815 **Figure 6.** Results for the dominant vegetation cover simulated by INLAND for the different treatments
 816 (A-L) and a metric of variability of results (a-l). Simulations are considered very robust if the dominant
 817 vegetation agrees on 9-10 of the last 10 years of simulation, robust if it agrees on 7-8 years, and
 818 transitional if on 6 or fewer years.

819

820



821 **Table 1.** Simulations with different scenarios evaluated by INLAND model in Amazonia-Cerrado
 822 transition. CA, climatological average, 1961-1990; CV, monthly climate data, 1948-2008; the nutrient
 823 limitation on V_{\max} - PC, no P limitation ($V_{\max} = 65 \mu\text{mol-CO}_2 \text{ m}^{-2} \text{ s}^{-1}$); PR, regional P limitation; PG,
 824 global P limitation).

Climate	CO ₂	Fire (F)	V_{\max}		
			PC	PR	PG
CA	Variable	Off	CA+PC	CA+PR	CA+PG
CA	Variable	On	CA+PC+F	CA+PR+F	CA+PG+F
CV	Variable	Off	CV+PC	CV+PR	CV+PG
CV	Variable	On	CV+PC+F	CV+PR+F	CV+PG+F

825

826



827 **Table 2.** Individual and combined effects for each simulation in Amazonia-Cerrado transition. CA,
 828 climatological seasonal average, 1961-1990; CV, monthly climate data, 1948-2008; the nutrient limitation
 829 on V_{\max} - PC, no P limitation ($V_{\max} = 65 \mu\text{molCO}_2 \text{ m}^{-2} \text{ s}^{-1}$); PR, regional P limitation; PG, global P
 830 limitation)

Climate (C)	Phosphorus (P)	Fire (F)
(CV+PC)-(CA+PC)	(CA+PR)-(CA+PC)	(CA+PC+F)-(CA+PC)
(CV+PR)-(CA+PR)	(CV+PR)-(CV+PC)	(CV+PC+F)-(CV+PC)
(CV+PG)-(CA+PG)	(CA+PG)-(CA+PC)	(CA+PR+F)-(CA+PR)
	(CV+PG)-(CV+PC)	(CV+PR+F)-(CV+PR)
		(CA+PG+F)-(CA+PG)
		(CV+PG+F)-(CV+PG)

831

832



833 **Table 3.** Summary of average NPP, LAI and AGB for the Amazonia-Cerrado transition at the transects
 834 domains, considering all simulations with CA and CV regardless of fire presence or P limitation. The
 835 results of a one-way ANOVA are also shown, including the F statistic, and p value. Values within each
 836 column followed by a different letter are significantly different ($p < 0.05$) according to the Tukey–Kramer
 837 test ($n=1860$: 31 pixels x 10 years x $n_{\text{simulation}/2}$).

Group 1	NPP		LAI_{total}		LAI_{lower}		LAI_{upper}		AGB	
	kg-C m ⁻² yr ⁻¹		m ² m ⁻²		m ² m ⁻²		m ² m ⁻²		kg-C m ⁻²	
CA	0.68	a	7.47	a	1.98	a	5.49	a	6.68	a
CV	0.64	b	7.15	b	2.11	a	5.04	b	6.30	b
F	40.2		57.2		2.96		36.0		11.3	
p	<0.001		<0.001		ns		<0.01		<0.001	

838

839



840 **Table 4.** Summary of average NPP, LAI and AGB for the transition at the transects domains, considering
 841 different P limitation, regardless of climate and fire presence. The results of a one-way ANOVA are also
 842 shown, including the F statistic, and p value. Values within each column followed by a different letter are
 843 significantly different ($p < 0.05$) according to the Tukey–Kramer test ($n=1240$: 31 pixels x 10 years x
 844 $n_{\text{simulation}}/3$).

Group 2	NPP		LAI _{total}		LAI _{lower}		LAI _{upper}		AGB	
	kg-C m ⁻² yr ⁻¹		m ² m ⁻²		m ² m ⁻²		m ² m ⁻²		kg-C m ⁻²	
PC	0.71	a	7.64	a	1.84	b	5.80	a	7.15	a
PR	0.64	b	7.15	b	2.19	a	4.95	b	6.20	b
PG	0.64	b	7.14	b	2.10	a	5.04	b	6.12	b
$F_{2,99}$	62.8		61.0		8.75		53.5		33.6	
p	<0.001		<0.001		<0.01		<0.01		<0.001	

845

846



847 **Table 5.** Summary of average NPP, LAI and AGB for the transition at the transects domains, considering
 848 presence or absence of fire. The results of a one-way ANOVA are also shown, including the F statistic,
 849 and p value. Values within each column followed by a different letter are significantly different ($p < 0.05$)
 850 according to the Tukey–Kramer test ($n=1860$: 31 pixels x 10 years x $n_{\text{simulation}/2}$).

Group 3	NPP		LAI _{total}		LAI _{lower}		LAI _{upper}		AGB	
	kg-C m ⁻² yr ⁻¹		m ² m ⁻²		m ² m ⁻²		m ² m ⁻²		kg-C m ⁻²	
Fire OFF	0.66	a	6.72	b	0.88	b	5.84	a	8.47	b
Fire ON	0.67	b	7.90	a	3.21	a	4.69	b	4.51	a
$F_{3,84}$	8.28		937		1459		249		1719	
p	<0.005		<0.001		<0.01		<0.01		<0.001	

851

852



853 **Table 6.** Summary of average NPP, LAI and AGB for the transition at the transects domains, considering
 854 all factor combinations. The results of a one-way ANOVA are also shown, including the F statistic, and
 855 p value. Values within each column followed by a different letter are significantly different ($p < 0.05$)
 856 according to the Tukey–Kramer test ($n=310$: 31 pixels x 10 years).

	NPP		LAI _{total}		LAI _{lower}		LAI _{upper}		AGB	
	kg-C m ⁻² yr ⁻¹		m ² m ⁻²		m ² m ⁻²		m ² m ⁻²		kg-C m ⁻²	
CV+PC	0.69	bcd	6.96	d	0.84	e	6.48	a	9.01	ab
CV+PG	0.61	f	6.24	f	0.85	e	5.60	bc	7.91	c
CV+PR	0.62	f	6.33	f	0.85	e	5.74	bc	8.04	c
CV+PC+F	0.69	abc	7.92	b	2.91	cd	4.61	ef	4.89	de
CV+PG+F	0.63	ef	7.76	b	3.73	a	5.81	bc	3.91	f
CV+PR+F	0.63	ef	7.65	bc	3.47	ab	4.69	ef	4.02	f
CA+PC	0.72	ab	7.39	c	0.91	e	6.12	ab	9.31	a
CA+PG	0.64	def	6.64	e	0.91	e	5.40	cd	8.22	c
CA+PR	0.65	cdef	6.72	de	0.91	e	5.49	cd	8.31	bc
CA+PC+F	0.74	a	8.29	a	2.69	d	5.02	de	5.40	d
CA+PG+F	0.67	cde	7.90	b	3.29	abc	4.04	g	4.45	ef
CA+PR+F	0.67	cde	7.88	b	3.19	bc	4.18	fg	4.42	ef
F	16.2		115		140		38.1		172	
p	<0.001		<0.001		<0.01		<0.01		<0.001	

857



858 **Table 7.** Correlation coefficients of AGB simulated by INLAND and field estimates (n= 310: 31 pixels
 859 x 10 years).

	T1	T2	T3	T4	T5	All transects
CA+PC	0.843	0.928	0.886	0.937	0.337	0.786
CV+PC	0.838	0.884	0.890	0.939	0.355	0.781
CA+PR	0.793	0.848	0.830	0.911	0.399	0.756
CV+PR	0.795	0.793	0.832	0.907	0.527	0.771
CA+PG	0.814	0.951	0.838	0.889	0.388	0.776
CV+PG	0.825	0.922	0.840	0.879	0.496	0.792
CA+PC+F	0.988	0.987	0.977	0.892	0.133	0.795
CV+PC+F	0.976	0.947	0.933	0.908	0.187	0.790
CA+PR+F	0.842	0.805	0.981	0.808	0.561	0.799
CV+PR+F	0.925	0.804	0.927	0.808	0.319	0.757
CA+PG+F	0.844	0.961	0.980	0.830	0.430	0.809
CV+PG+F	0.845	0.932	0.931	0.881	0.177	0.753
CA avg	0.854	0.913	0.915	0.878	0.375	0.787
CV avg	0.867	0.880	0.892	0.887	0.344	0.774

860